

UDC 544.7

O. O. Streltsova, G. M. Dzhyga, A. F. Tymchuk

Odesa I. I. Mechnikov National University,

Faculty of Chemistry and Pharmacy, Department of Physical and Colloid Chemistry,

2 Zmiienska Vsevoloda St, Odesa, 65082, Ukraine;

e-mail: Tymchuk@onu.edu.ua

STUDY OF ADSORPTION MECHANISM OF CATIONIC SURFACTANTS BY BENTONITE FROM ASKAN DEPOSIT

Adsorption of cationic surfactants — dodecylammonium chloride and hexadecylpyridinium perchlorate from aqueous solutions by the natural bentonite from Askan deposit of Georgia was studied. The microstructural parameters and surfactant loading and distribution, were determined by X-ray diffraction and analysis of FT-IR spectra. The objective was to improve the understanding of the behaviour of surfactants when adsorbed by bentonite for its possible use as antimicrobial preparations. The adsorption constants from the Langmuir, Freundlich and Dubinin-Radushkevich equations were used to compare the adsorption of surfactants by bentonite. The obtained high values of the Gibbs free energy of adsorption indicate a high affinity of cationic surfactants to bentonite. The kinetics of the adsorption process was analysed using the kinetic models of pseudo-first and pseudo-second order, intraparticle diffusion, intraparticle diffusion of Boyd and Weber-Morris. It was found that the degree of adsorption from the studied surfactants by bentonite reaches 70–80%.

Keywords: cationic surfactant, bentonite, adsorption, kinetics.

INTRODUCTION

The development of combined action pharmaceuticals is a pressing issue due to the increasing risks of man-made impacts on humans and the environment. Such preparations include antibiotics, surfactants, natural and synthetic recipients. A number of antimicrobial preparations containing alkylpyridinium salts, quaternary ammonium salts and other cationic surfactants [1–3] have been developed. They have high sorption capacity, biological activity, antibacterial and disinfectant properties. Combining cationic surfactants with bentonite, kaolin and other natural sorbents significantly enhances their effectiveness. The study of such systems expands the capabilities of pharmaceutical technologies in the field of antimicrobial drug production. Bentonite clays are promising materials [4, 5], the use of which makes adsorption especially attractive from a medical and economic point of view. On the one hand, the presence of a cation exchange capacity in them can be used for the adsorption of surfactants by minerals, stabilization of colloids and nanoparticles, in chemical and pharmaceutical synthesis etc. [6, 7] On the other hand, surface modification of minerals with organic cations opens up the possibility of obtaining systems with certain controllable properties [8, 9]. The results of SEM systems cetyltrimethylammonium bromide-modified bentonite (CTAB-MB) illustrated the few number particles in agglomerates of bentonite compared to modified bentonite [10]. According these results, the CTAB-MB was obtained efficient adsorbent to remove the Methylene Blue. Experience has shown [4, 11], that adsorption surfactants by clays is the effectively. In many cases, the process depends not only on the nature of the surfactant, but also on the structure of clay minerals and,

This is an open access article under the Creative Commons Attribution 4.0 International (CC BY 4.0) license.

[https://doi.org/10.18524/2304-0947.2025.2\(90\).352382](https://doi.org/10.18524/2304-0947.2025.2(90).352382)

© O. O. Streltsova, G. M. Dzhyga, A. F. Tymchuk, 2025

as a consequence, on their physicochemical properties [4, 12–15]. Today, many studies have been carried out concerning the adsorption of surfactants on clay minerals in order to clarify the mechanism of adsorption [4, 16–23]. The authors [18] established the dependence adsorption of surfactants by clay minerals, which decreased in the following order: cationic (octadecyltrimethylammonium bromide) > nonionic (Triton X-100) > anionic (sodium dodecylsulfate). Almost all clay minerals showed a high adsorption capacity with respect to the cationic surfactant.

The formation of organo-clays has been characterized by several additional methods (adsorption isotherms, XRD and IR spectroscopy). Guégan, R. *et al.* [22] studied the adsorption of benzyltrimethyltetradecylammonium chloride (BDTAC), a cationic surfactant, and triethylene glycol monodecyl ether (C10E3), a nonionic surfactant by Ca-smectite. They reported that BDTAC was ion exchanged in stoichiometric proportions with the Ca^{2+} counterions. For surfactants, expansion was limited to two adsorbed monolayers parallel to the clay surface. The authors [23] showed that the adsorption of cetylpyridinium chloride and cetyltrimethylammonium bromide on clays with a high Na^+ content is well described by the Langmuir, Freundlich, and Langmuir-Freundlich models. These results indicate a monolayer arrangement of both surfactants on the outer surface of montmorillonite. Authors [24] investigated the effect of the adsorption of cationic surfactant, hexadecyltrimethylammonium bromide (HDTMA), on the structure of bentonite. The organo-bentonites as applicator as sorbents were evaluated. It was shown that the morphology of the sample after the modification with HDTMA did not change significantly.

The mathematical processing of adsorption isotherms surfactants was carried out according to the Langmuir equation and the constants of adsorption equilibrium, limiting adsorption, and Gibbs free energy were found. Adsorption isotherms, kinetics, thermodynamics, as well as additional interactions are compared and considered in detail by the authors [24–26] In addition, the limitations, differences and directions of the use of clay adsorbents are discussed. The adsorption equilibrium is explained by the isotherms of Langmuir, Freundlich, Redlich-Peterson, Dubinin-Radushkevich, Temkin, Thoth, Hill [26].

Kinetic studies are important to determine the optimal conditions for adsorption. Usually, the experimentally obtained kinetic regularities of adsorption of organic substances are analysed by comparing them with theoretical kinetic models [4, 26]. To study the adsorption of surfactants by montmorillonite, the typical Lagergren pseudo-first order kinetic model and the McKay pseudo-second order kinetic model were applied [27] It was shown that the distribution of the total adsorption capacity of surfactant in the layers and on the surface of montmorillonite corresponds to the result of adsorption and is modelled by a pseudo-second order kinetic model. Unfortunately, the information available in literature on the application of different kinetic models to describe the adsorption of surfactants on bentonites is scarce and contradictory [4, 8, 13, 26–29].

An analysis of scientific literature in the field of research into systems containing surfactants together with natural sorbents has confirmed their abundance. However, the need to study and develop effective broad-spectrum biomedical preparations including surfactants find clays remains relevant. The aim of this work was to study the adsorption of some cationic surfactants by the natural bentonite from Askan deposit and to elucidate the mechanism of the process.

EXPERIMENTAL

Materials

In this study used natural bentonite (N-Bent) from Askan deposit (Georgia) with the following chemical composition (wt%): SiO₂ — 51.0; Al₂O₃ — 16.86; Fe₂O₃ — 3.29; MgO — 2.64; CaO — 2.07; Na₂O — 0.65; K₂O — 0.50; TiO₂ — 0.25. The cation exchange capacity (CEC) of the bentonite, which was determined by the methylene-blue adsorption titration method, 35 meq/100 g. Prior to the experiments, the samples were air-dried, sieved through a 2 mm sieve, and thoroughly crushed in the agate mortar. For all experiments, only the fraction containing a grain size of <0.2 mm was used. The dodecylammonium chloride, DDAC (C₁₂H₂₈ClN) and hexadecylpyridinium perchlorate, HDPP (C₂₁H₃₈NClO₄) was purchased from Sigma-Aldrich (Germany). They were analytical grade and used without further purification.

Methods

The X-ray diffraction powder analysis was carried out on a Siemens D500 diffractometer (CuK α radiation, $\lambda = 1.54178 \text{ \AA}$) with a secondary beam graphite monochromator. Analysis of FT-IR spectra in the range from 400 to 4000 cm⁻¹ with resolution of 4 cm⁻¹ was carried out using a Perkin Elmer FT-IR spectrometer. All spectra were recorded using pellets consisting of 1 mg of the material under study and 200 mg of KBr compressed under pressure of 7 t/cm² for 30 s.

The method of studying adsorption was as follows. The masses (0.03 g) of the bentonite placed in Erlenmeyer flasks with a volume of 50 cm³, which contain 25 cm³ of surfactants solutions by concentrations $(2.0\text{--}40.0) \times 10^{-5} \text{ mol/L}$, placed on a shaker for stirring for 30 min (this time was sufficient to establish adsorption equilibrium in the system) at a temperature of 293 K in a Julabo MC-4 thermostat, that allowed to maintain the desired temperature with precision to 0.001K. After the adsorption is completed, the adsorbent is separated from the equilibrium solution by centrifuged at 50 rpm using a CLS-3 laboratory centrifuge. The solution separated from the adsorbent was analysed for its surfactant content.

The analysis of solutions for residual content of dodecylammonium chloride and hexadecylpyridinium perchlorate before and after adsorption was carried out photocolourimetry by standard techniques [30] respectively. The samples after adsorption were denoted as DDAC-N-Bent and HDPP-N-Bent.

Adsorption degree of surfactants (S , %) was determined as Eq.(1).

$$S = \frac{C_0 - C}{C_0} \cdot 100 \quad (1)$$

where C_0 and C are concentrations of the solution before and after adsorption.

Adsorption capacity (A , mol/g) was calculated as Eq. (2).

$$A = \frac{C_0 - C}{m} \cdot V \quad (2)$$

where V is the solution volume; m is the mass of weighted sample.

Phase compositions

XRD patterns of natural bentonite and bentonites after adsorption of cationic surfactants are shown in Fig.1. X-ray spectral parameters for N-Bent, DDAX-N-Bent, and HDPP-N-Bent are presented in Table 1. By identification of XRD patterns, it has been found that this bentonite is polyphase mineral containing montmorillonite (M) (layered aluminosilicate with 2:1 structure), α -quartz (Q), muscovite (Ms), kaolinite (K), albite (A) and calcite (C). The main phase of montmorillonite was identified in the natural bentonite samples at the following values of angles of reflection, 2θ , and inter-planar spacing (d , Å): 6.243° (14.146) – 19.719° (4.498) – 34.559° (2.593) – 54.900° (1.671).

The value of the first basal distance of the montmorillonite phase d_{001} (Fig. 1) in the samples of the natural bentonite has low intensity and it is hard to notice. The reason may be the low crystallinity of the montmorillonite phase in the investigated sample. After treatment by DDAC and HDPP, the basal reflection of clay-Na shifted slightly to higher values depending on nature of the surfactants. The value of the first basal distance of the montmorillonite phase d_{001} in the samples after adsorption of surfactants (DDAC-N-Bent and HDPP-N-Bent) caused a slight expansion of the interlayer space of montmorillonite (14.14–14.25 Å). Also, after the adsorption of a surfactant by bentonite, the formation of new phases due to surfactant molecules is not observed. This could be due to the low concentration of the surfactant ($c_{\text{surf}} = 15.0 \cdot 10^{-5}$ mol/L) and that the molecule of DDAC and HDPP is too big to intercalate between the interlayer space; therefore, expansion of the interlayer space was not significant, and the sorption of cationic surfactants on bentonite was seen mostly on the surface. These findings align with findings from other studies [8, 32] and, as a consequence, on the physical nature of the adsorption process.

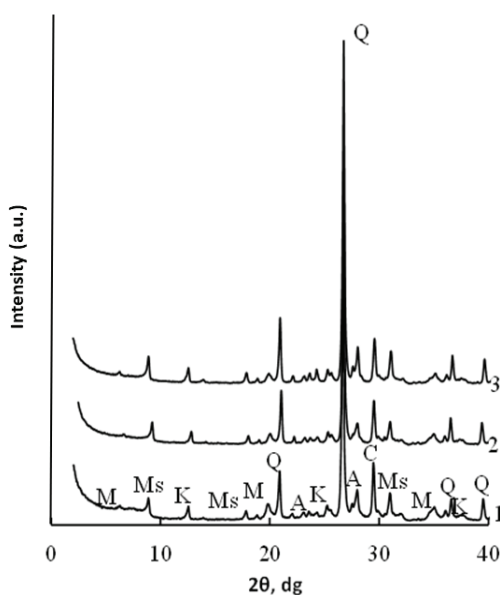


Fig. 1. X-ray diffraction patterns for N-Bent (1), DDAC-N-Bent (2), HDPP-N-Bent (3)

Table 1

**X-ray spectral parameters for natural bentonite
and bentonites after adsorption of cationic surfactants**

Phase	2 θ , dg	d, Å	2 θ , dg	d, Å	2 θ , dg	d, Å	d, Å ref. data
	N-Bent		DDAC-N-Bent		HDPP-N-Bent		
Mont (M)	6.243	14.146	6.230	14.253	6.233	14.248	15.540
	19.719	4.498	19.707	4.501	19.701	4.502	4.490
	61.680	1.502	61.650	1.503	61.711	1.501	1.500
α -SiO ₂ (Q)	20.863	4.254	20.867	4.253	20.866	4.253	4.250
	26.651	3.342	26.653	3.341	26.653	3.341	3.350
	50.165	1.817	50.167	1.817	50.168	1.817	1.820
Muscovite (Ms)	18.804	4.715	18.794	4.717	18.805	4.715	4.720
	30.983	2.884	30.813	2.899	30.884	2.893	2.860
Kaolinite (K)	12.504	7.073	12.498	7.076	12.505	7.072	7.140
	25.161	3.536	25.148	3.538	25.163	3.536	3.550
Albite (A)	23.522	3.779	23.537	3.776	23.535	3.777	3.700
	27.900	3.195	27.936	3.191	27.927	3.192	3.210
Calcite (C)	29.518	3.023	29.528	3.022	29.563	3.019	3.030
	47.572	1.909	47.579	1.909	47.576	1.909	1.912

FT-IR spectral investigations

Fig. 2 shows FT-IR spectra for N-Bent, DDAC-N-Bent, DDAC, HDPP-N-Bent and HDPP. The polyphase composition of this natural bentonite was confirmed by IR spectral data. This is evident from the bands characteristic of the main montmorillonite phase in the region of stretching (ν) and deformation (δ) vibrations of its structural groups as well as the bands assigned to impurities, i.e. kaolinite, α -quartz, and calcite. Interpretation of FT-IR spectra for N-Bent (Table 2) was carried out by their comparison with the data reported [12, 22].

Analysing the FT-IR spectra in the range of stretching and deformation vibrations of OH groups bound with octahedral cations and OH groups in the associated water molecules, we can notice that a band characteristic of Al–Al–OH is clearly defined; a band at 915 cm⁻¹ is registered only as a bend. The presence of a characteristic the band shows that N-Bent contains a kaolinite phase. The bands visible at the 3429 cm⁻¹ and 1630 cm⁻¹ region correspond with H–O–H vibrations in water (stretching vibrations and deformation vibrations, accordingly). Major bands in the 1034–468 cm⁻¹ region are ascribed to bond vibrations in the structure of the examined mineral and are associated with the vibration of Si–O–Si (1034 cm⁻¹ and 468 cm⁻¹) and Si–O–Al bridges (520 cm⁻¹). A band at 874 cm⁻¹ can be assigned to deformation vibrations of OH groups

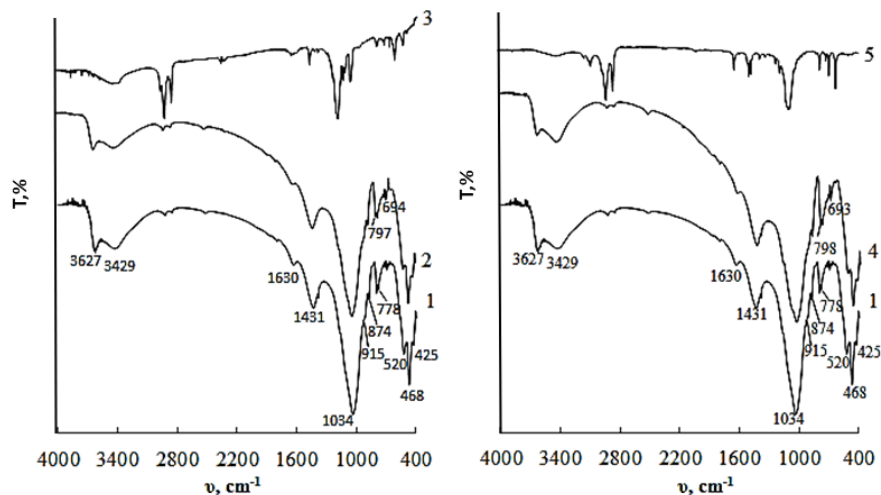


Fig. 2. FT-IR spectra N-Bent (1), DDAC-N-Bent (2), DDAC (3), HDPP-N-Bent (4) and HDPP (5)

Table 2

Wave numbers (cm^{-1}) for absorption maxima in FT-IR spectra of N-Bent, DDAC-N-Bent, and HDPP-N-Bent

Structural group	N-Bent		DDAC-N-Bent		HDPP-N-Bent	
	ν	δ	ν	δ	ν	δ
Al–Al–OH	3627	915 bend	3625	918 bend	3623	918 bend
Al–Fe ³⁺ –OH	–	874	ν	875	–	875
H ₂ O	3429	1630	3420	1628	3426	1621
Si–O–Si (tetrahedron)	1034	468	1033	470	1032	467
Si–O–Al	–	520	–	519	–	517
Si–O–Mg	–	425	–	425	–	426
α -SiO ₂ (α -quartz)	–	797, 778, 695	–	797, 778, 693	–	798, 779, 693
CO ₃ ²⁻	–	1431	–	1430	–	1428

in Al–Fe³⁺–OH structural fragments. The presence of a characteristic doublet at 797 cm^{-1} and 778 cm^{-1} shows that N-Bent contain an α -quartz phase. Compared to N-Bent spectrum, organoclays spectra the main peaks of clay with three supplementary peaks around 2920, 2850, and 1470 cm^{-1} that were referred to C–H stretching bands of —CH₂, aliphatic C–H stretch and aromatic C=C vibrations. These bands approved both the conservation of starting clay structure and the loading of DDAC and HDPP into clay. These bands are sensitive to the packing density of the methylene chain as well as the surfactant loading [28].

Protolytic properties

It is known that the amount of adsorption of cationic surfactants on polar adsorbents depends on pH [12]. When studying the protolytic properties of natural bentonite, it was established equilibrium pH, pH_{eq} , values are quickly attained and stay unchanged for long period of time. Interaction between water molecules and a bentonite surface results in the formation of alkaline medium ($\text{pH} = 7.98$).

Kinetics of adsorption

The studies carried out have shown (Fig. 3) that the time to achieve adsorption equilibrium between an aqueous solution of HDPP, DDAC and bentonite have small depends on the nature of the surfactant and is achieved in 14–15 minutes of joint shaking. The adsorption degree (S, %) of DDAC is 80%, while in the case of HDPP this figure is 68% (Fig. 3). This is due to the different structure of the surfactant.

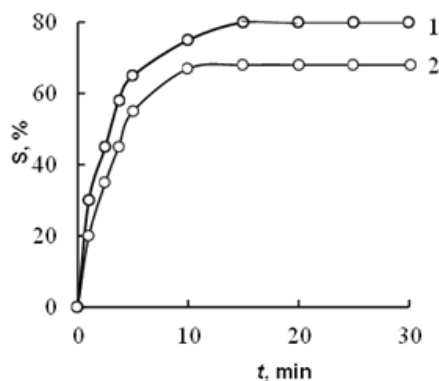


Fig. 3. Adsorption degree of cationic surfactants by bentonite from aqueous solutions over time. Sorbent dosage was 0.6 g/L; 1 — DDAC; 2 — HDPP. $C_{\text{surf}} = 50 \text{ mg/L}$; $V = 0.05 \text{ L}$; $T = 293 \text{ K}$

It is known that the theoretical processing of kinetic curves using the models of diffusion and chemical kinetics enables one to determine the adsorption mechanism and the rate-limiting steps of the process. In this study, the kinetics of the adsorption process was analysed using the pseudo-first [31], pseudo-second order [32], kinetic models and intraparticle diffusion [33], intraparticle diffusion of Boyd and Weber-Morris. To determine the values of the parameters of these models, a minimization procedure was carried out using the Origin Lab Pro mathematical package [34]. To establish a model that optimally describes the adsorption of surfactants on bentonite, we compared the correlation coefficients R^2 for each surfactant. The results of processing the integral kinetic curves of surfactant adsorption by bentonite using chemical kinetic models are shown in Table 3.

The linear form of pseudo-first and pseudo-second order model equation can be expressed, respectively, by Eqs. (3, 4).

$$\ln(A_e - A) = \ln A_e - k_1 t \quad (3)$$

$$\frac{t}{A} = \frac{1}{k_2 A_e^2} + \frac{1}{A_e} t, \quad (4)$$

where A_e and A are the amounts of the surfactants on the adsorbent at equilibrium and various time t , respectively; k_1 , k_2 is the adsorption rate constant of pseudo-first and pseudo-second order model.

Fig. 4 (*a, b*) shows the kinetics of cationic surfactants adsorption by natural bentonite in the coordinates of the pseudo-first and pseudo-second order models. The correlation coefficients calculated for the pseudo-second order kinetic model ($R^2 = 0.99$) and also the good agreement of calculated values of A_e^{calc} and experimental values of A_e^{exp} indicate that the adsorption systems follow the pseudo-second order kinetic model (Table 3).

Table 3

Kinetic parameters for the adsorption of surfactants by bentonite

Kinetic parameters	Adsorbate solution	
	DDAC	HDPP
$A_e^{\text{exp}} \cdot 10^4, \text{ mol/g}$	2.55	1.15
Pseudo-first order		
$A_e^{\text{calc}} \cdot 10^4, \text{ mol/g}$	1.91	0.95
$k_1, \text{ min}^{-1}$	0.23	0.61
R^2	0.92	0.95
NSD, %	30.30	30.26
Kinetic parameters	Adsorbate solution	
	DDAC	HDPP
Pseudo-second order		
$A_e^{\text{calc}} \cdot 10^4, \text{ mol/g}$	2.73	1.18
$k_2 \cdot 10^{-3}, \text{ g/mol} \cdot \text{ min}$	2.06	14.1
R^2	0.99	0.99
NSD, %	2.45	2.00
Intrafilm diffusion		
$k_{\text{film}}, \text{ min}^{-1}$	0.41	0.63
R^2	0.95	0.99
NSD, %	5.10	0.60
Intraparticle diffusion of Boyd		
$B, \text{ min}^{-1}$	0.42	0.61
R^2	0.89	0.99
NSD, %	2.70	0.60

This equation makes it possible to take into account not only the adsorbent– adsorbate interactions, but also the intermolecular interactions of adsorbed substances [29] which determine the high adequacy of the use of the second-order kinetic model. On the contrary, when the pseudo-first order model is used, the linear correlation coefficients of the straight lines appear to be smaller and the experimental and calculated values of equilibrium adsorption turn out to be significantly different.

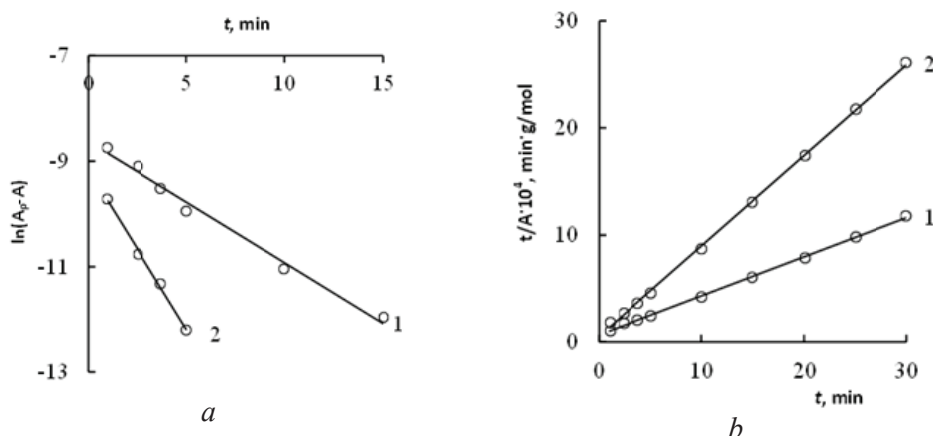


Fig. 4. Application of the model of chemical reaction of pseudo-first (a) and pseudo-second order (b): 1 — DDAC; 2 — HDPP

To determine the rate-limiting step of the adsorption process, the integral kinetic curves were processed using equations for intrafilm and intraparticle diffusion kinetics [35]. The linear form of intrafilm diffusion, intraparticle diffusion of Boyd and Weber-Morris equation can be expressed, respectively, by Eqs. (5–7).

$$\ln\left(1 - \frac{A}{A_e}\right) = -k_{film} \cdot t \quad (5)$$

$$\ln\left(1 - \frac{A}{A_e}\right) = \ln \frac{6}{\pi^2} - B \cdot t \quad (6)$$

$$A = k_{W-M} \cdot t^{1/2} + I \quad (7)$$

where k_{film} is the rate constant of the intrafilm diffusion (s^{-1}); B is the rate constant of the intraparticle diffusion of Boyd (s^{-1}); k_{W-M} is the rate constant of the intraparticle diffusion of Weber-Morris ($\text{mmol/g} \cdot \text{min}^{1/2}$); I is the Y-intercept (mmol/g).

Studies of the adsorption of cationic surfactants by bentonite using diffusion models have shown that the form of the dependence curves $\ln(1 - A/A_e) = f(\tau)$ shown in Fig. 5a and Fig. 5b indicates the effect of film diffusion on the adsorption process. In

the initial part of the curve, a nonlinear dependence of the change in adsorption on time is observed. The dependencies $A-\tau^{1/2}$ in the coordinates of the Morris-Weber equation (Fig. 5c) for the adsorption of surfactants on bentonite are not linear, which indicates a mixed diffusion mechanism of adsorption kinetics, when the process cannot be unambiguously limited by external or internal diffusion.

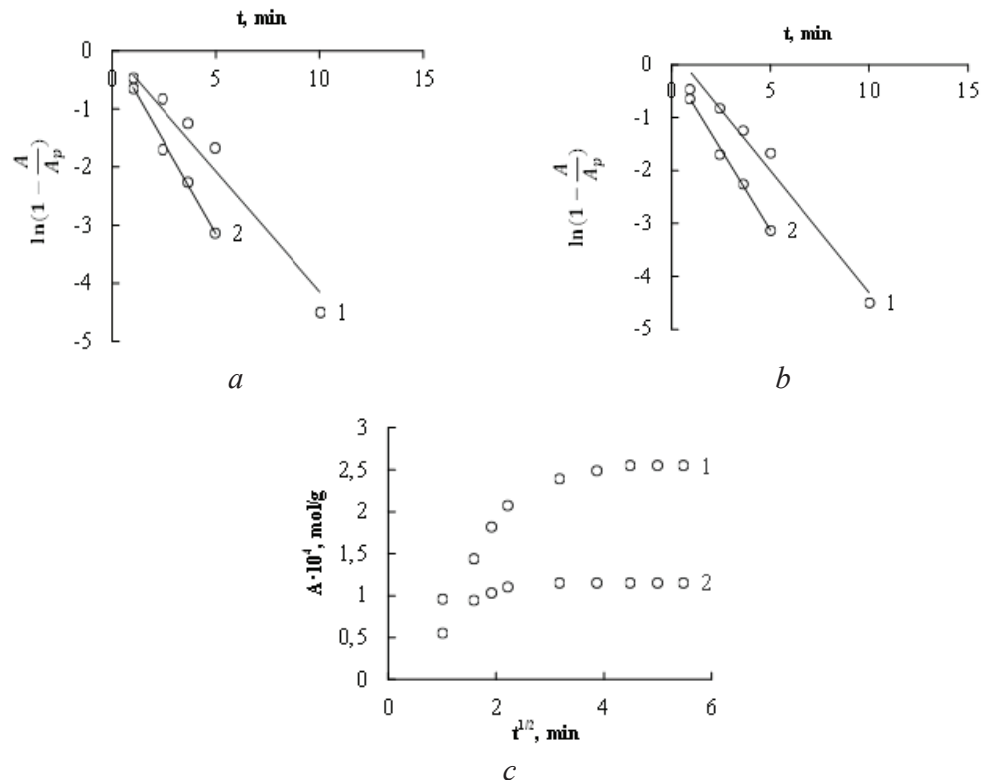


Fig. 5. Application of the model of intrafilm diffusion (a), intraparticle diffusion of Boyd (b) and Weber-Morris (c): 1 — DDAC; 2 — HDPP

As can be seen from Fig. 5c, the kinetic curves for the adsorption of cationic surfactants by natural bentonite are described by straight lines in the A versus $\tau^{1/2}$ coordinates only at an initial stage of the adsorption. Therefore, within a period of 0–10 min, the intrafilm diffusion (diffusion in the solution film) is the rate-limiting step, which determines the total rate of the process. The subsequent deviation from the rectilinear $A = f(\tau^{1/2})$ dependence indicates that the influence of the intrafilm diffusion weakens, while the effect of the intraparticle diffusion become stronger.

The results of calculations and comparison of the numerical values of the rate constants of external and internal diffusion confirm the mixed-diffuse nature of the kinetics of the adsorption of surfactants by natural bentonite.

Adsorption isotherms

To clarify the adsorption mechanism the experimentally obtained adsorption isotherms are analysed. Fig. 6 shows the isotherms of adsorption of DDAC and HDPC by natural bentonite. The adsorption isotherms of cationic surfactants compounds may be attributed to L-type isotherms according to the Giles classification. In both cases, in the initial section of the isotherms, adsorption increases linearly with an increase in the surfactant concentration, which indicates the adsorption of the surfactant due to the electrostatic interaction of the adsorbate with the adsorbent. A further increase in the surfactant concentration leads to an increase in the mutual attraction of the surfactant hydrocarbon radicals, to the start of association in the adsorption layer (association also occurs in the total solution volume), and adsorption increases.

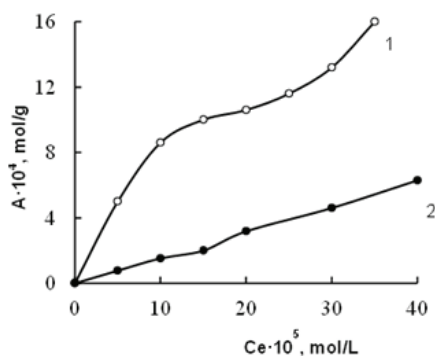


Fig. 6. Adsorption isotherms of cationic surfactants by natural bentonite:
1 — DDAC; 2 — HDPP. T = 298 K, q = 0.6 g/L

For modelling of the adsorption isotherm models of Langmuir, Freundlich and Dubinin-Radushkevich were used [35]. The linear form of isotherms is represented by Eqs. (8–10).

$$\text{Langmuir isotherm: } \frac{C}{A} = \frac{1}{K_L A_\infty} + \frac{1}{A_\infty} C \quad (8)$$

$$\text{Freundlich isotherm: } \ln A = \ln K_F + \frac{1}{n} \ln C \quad (9)$$

$$\text{Dubinin-Radushkevich: } \ln A = \ln A_{D-R} - K_{D-R} R^2 T^2 \left[\ln \left(1 + \frac{1}{C} \right) \right]^2 \quad (10)$$

where A is the equilibrium static capacity; C is the equilibrium concentration of surfactants in solution; A_∞ is the amount of adsorbate at complete monolayer coverage; K_L is the Langmuir constant that relates to the energy of adsorption; K_F is the measure of adsorption capacity; $1/n$ is the adsorption intensity; A_{D-R} is maximum adsorption capacity of the adsorbent; K_{D-R} is the Dubinin-Radushkevich constant.

Characteristic energy of adsorption (E) was calculated according with Eq. (11).

$$E = \frac{1}{(2K_{D-R})^{1/2}} \quad (11)$$

Standard free energy of the adsorption (ΔG^0) was calculated according with Eq. (12).

$$\Delta G^0 = -RT \ln K_L \quad (12)$$

For the modelling of the adsorption the corresponding coefficient of determination R^2 , deviation percentage (NSD, %) were used Eq. (13).

$$NSD = 100 \cdot \frac{\sum_{i=1}^N |A_i^{\text{calc}} - A_i^{\text{exp}}|}{\sum_{i=1}^N A_i^{\text{exp}}} \quad (13)$$

In a typical approach, the two-parameter Langmuir and Freundlich models are employed to fit adsorption isotherms. The Langmuir model suggests that adsorption occurs on a homogeneous surface without any lateral interactions between adsorbed molecules. The Freundlich model is widely used to describe adsorption on a surface with a heterogeneous energy distribution, accompanied by possible interactions between adsorbed molecules. It was found that the Langmuir equation describes the experimental adsorption isotherms of DDAC with bentonite in the region of filling the monolayer (Fig. 7). It was found that the value of the limiting adsorption of HDPP is less than that of DDAC, which is associated with the hindered adsorption of HDPP due to steric effects (Table 4). The K_L values are significant $((1.01-3.85) \cdot 10^5, \text{L/mol})$, that is typical for systems with increased adsorption selectivity. The obtained high values of the Gibbs free energy of adsorption ΔG^0 indicate a high affinity of cationic surfactants to bentonite and confirm the physical nature of adsorption, when weakly adsorbed water molecules are displaced from the adsorption layer by strongly adsorbed surfactant molecules and ions, and determines the advisability of using this natural bentonite for the extraction of DDAC and HDPP from aqueous solutions.

Freundlich's equation, according to an additional trend in the Excel program with high accuracy ($R^2 = 0.98$), has shown its suitability for describing the middle area of concentration of isotherms of adsorbed HDPP (Table 4). The specific features of the adsorption isotherms of the surfactants under study are reflected in the value of the parameter n , the value of which agrees with the ordering coefficient α (Hildebrand's equation [36]) and indicates the ideal nature of adsorption ($n > 1$). As the surface is filled, the binding energy of the adsorbent-adsorbate decreases. All obtained isotherms in the entire range of equilibrium surfactant concentrations are described by the Dubinin-Radushkevich equation (Fig. 7, Table 4) with high values of the linear correlation coefficients. The values of the characteristic adsorption energy DDAC by bentonite indicate the contribution of ion exchange to the adsorption mechanism. Contradicts the calculations made on the basis of the Langmuir and Freundlich models and the conclusions drawn from the analysis of FT-IR spectra. This fact requires further confirmation using higher concentrations of surfactants.

Table 4

**Constants of equations characterizing adsorption
of cationic surfactants by natural bentonite**

Constants of adsorption equations	Adsorbate solution	
	DDAC	HDPP
Langmuir equation		
$A_{\infty} \cdot 10^4, \text{ mol/g}$	20.00	9.47
$K_L \cdot 10^{-5}, \text{ L/mol}$	3.85	1.01
$-\Delta G^0, \text{ kJ/mol}$	31.32	28.08
R^2	0.96	0.85
Freundlich equation		
$K_F, \text{ mol}^{(1-1/n)} \text{ L}^{1/n}/\text{g}$	0.03	1.43
n	2.56	1.04
R^2	0.93	0.98
Dubinin-Radushkevich equation		
$A_{D-R} \cdot 10^4, \text{ mol/g}$	84.1	193.0
$K_{D-R} \cdot 10^0, \text{ mol}^2/\text{J}^2$	4.15	8.55
$E, \text{ kJ/mol}$	10.98	7.65
R^2	0.96	0.98

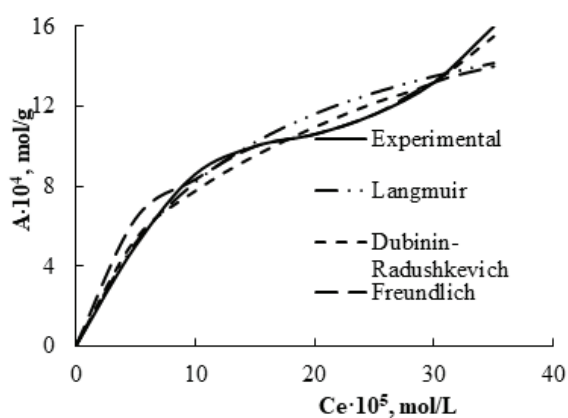


Fig. 7. Comparison of experimental isotherms of DDAC adsorption by bentonite with those calculated theoretically by the Langmuir, Freundlich and Dubinin-Radushkevich models

A graphical comparison of the experimental and theoretical adsorption isotherms calculated using the constants of the Freundlich, Langmuir, and Dubinin-Radushkevich models (using the example of Fig. 7) showed that the experimental adsorption isotherms are described by the Langmuir and Dubinin-Radushkevich equations in a wider concentration range than the Freundlich equation.

CONCLUSION

The adsorption of cationic DDAC and HDPP from aqueous solutions by natural bentonite of the Askan deposit was studied. The morphology and structure of interlayers in the sample of bentonite adsorbed surfactants and the non-adsorbed sample were investigated by X-ray diffraction and IR spectroscopy, respectively. The results showed that after the adsorption of cationic surfactants by natural bentonite, no special changes and formation of new phases due to surfactant molecules are observed, which is due to the low content of these substances. The extent of adsorption depends on the surfactant concentration. The highest value (80%) was achieved for DDAC at an initial concentration of 50 mg/L. Surfactant uptake by organo-modified clays can be explained by two processes: adsorption onto the clay surfaces and intercalation into the clay layers. This was confirmed by X-ray diffraction and IR spectroscopy. On the basis of processing the experimental data within the framework of chemical kinetics and diffusion models, as well as the Langmuir, Freundlich and Dubinin-Radushkevich adsorption equations, a mechanism of adsorption of the studied surfactants was proposed. Calculations showed that the adsorption process corresponds to the kinetic model of pseudo-second order. The adsorption process occurs in the region of mixed diffusion, controlled by both internal and external diffusion, which is due to the layered structure of the adsorbent. Analysis of the data using adsorption models showed that the Langmuir and Dubinin-Radushkevich models interpret the experimental data better than the Freundlich model. The adsorption process carried out under optimal conditions provides a high degree of adsorption of DDAC and HDPP. Based on the obtained data, it can be concluded that natural bentonite from Askan deposit is highly efficient and suitable for combined use with cationic surfactants in compositions with antimicrobial properties.

REFERENCES

1. Parfitt G. D., Rochester C. H. Adsorption from solution at the solid/liquid interface. London: Academic Press, 1983. 416 p.
2. Sajid M., Nazal M., Baig N., Osman A. M. Removal of heavy metals and organic pollutants from water using dendritic polymers based adsorbents: a critical review. *Sep. Purif. Technol.* 2018, 191, 400–423. <https://doi.org/10.1016/j.seppur.2017.09.011>
3. Siyal A. A., Shamsuddin M. R., Low A., Rabat N. E. A review on recent developments in the adsorption of surfactants from wastewater. *J. Environ. Manage.* 2020, 254, 109797. <https://doi.org/10.1016/j.jenvman.2019.109797>
4. Awad A. M., Shaikh S. M., Jalab R., Gulied M. H., Nasser M. S., Benamor A., Adham S. Adsorption of organic pollutants by natural and modified clays: a comprehensive review. *Sep. Purif. Technol.* 2019, 228, 115719. <https://doi.org/10.1016/j.seppur.2019.115719>
5. Ying G. G., Guang-Guo Y. Fate, behaviour and effects of surfactants and their degradation products in the environment. *Environ. Int.* 2006, 32(3), 417–431. <https://doi.org/10.1016/j.envint.2005.07.004>
6. Seweryn A. Interactions between surfactants and the skin – Theory and practice. *Adv. Colloid Interface Sci.* 2018, 256, 242–245. <https://doi.org/10.1016/j.cis.2018.04.002>
7. Rosen M. J., Kunjappu J. M. Surfactants and interfacial phenomena. Hoboken, NJ: Jon Willey and Sons, Inc., 2012. 616 p.
8. Andrunik M., Bajda T. Modification of bentonite with cationic and nonionic surfactants: structural and textural features. *Materials.* 2019, 12(22), 3772. <https://doi.org/10.3390/ma12223772>
9. Shen T., Gao M. Gemini surfactant modified organo-clays for removal of organic pollutants from water. *Chem. Eng. J.* 2019, 375, 121910. <https://doi.org/10.1016/j.cej.2019.121910>
10. Khan M. N., Zareen U. Sand sorption process for the removal of sodium dodecyl sulfate (anionic surfactant) from water. *J. Hazard. Mater.* 2006, 133(1–3), 269–275. <https://doi.org/10.1016/j.jhazmat.2005.10.031>

11. Junin R., Amirian T., Idris A. K. Adsorption of nonionic surfactants on clay minerals. *J. Teknol.* 2011, 56(1), 113–122. <https://doi.org/10.11113/jt.v56.904>
12. Tarasevich Y. I., Ovcharenko F. D. Adsorbtsiya na glinistykh mineralakh [Adsorption on clay minerals]. Kyiv: Naukova dumka, 1975. 352 p. [in Russian].
13. Yang K., Zhu L., Xing B. Sorption of sodium dodecylbenzene sulfonate by montmorillonite. *Environ. Pollut.* 2007, 145(2), 571–576. <https://doi.org/10.1016/j.envpol.2006.04.024>
14. Li N., Xu L., Xu G., Sun W., Yu S. Simple synthesis of Cu₂O/Na-bentonite composites and their excellent photocatalytic properties in treating methyl orange solution. *Ceram. Int.* 2016, 42(5), 5979–5984. <https://doi.org/10.1016/j.ceramint.2015.12.145>
15. Vinuth M., Naik H. S. B., Vinoda B. M., Gururaj H., Thomas N., Arunkumar G. Enhanced removal of methylene blue dye in aqueous solution using eco-friendly Fe(III)–montmorillonite. *Mater. Today Proc.* 2017, 4(2A), 424–433. <https://doi.org/10.1016/j.matpr.2017.01.041>
16. Hong R., Guo Z., Gao J., Gu C. Rapid degradation of atrazine by hydroxyl radical induced from montmorillonite templated subnano-sized zero-valent copper. *Chemosphere.* 2017, 180, 335–342. <https://doi.org/10.1016/j.chemosphere.2017.04.025>
17. Khataee A., Kiransan M., Karaca S., Sheydaei M. Photocatalytic ozonation of metronidazole by synthesized zinc oxide nanoparticles immobilized on montmorillonite. *J. Taiwan Inst. Chem. Eng.* 2017, 74, 196–204. <https://doi.org/10.1016/j.jtice.2017.02.014>
18. Sánchez-Martín M. J., Dorado M. C., Del Hoyo C., Rodríguez-Cruz M. S. Influence of clay mineral structure and surfactant nature on the adsorption capacity of surfactants by clays. *J. Hazard. Mater.* 2008, 150(1), 115–123. <https://doi.org/10.1016/j.jhazmat.2007.04.093>
19. Komadel P., Madejová J. Chapter 7.1. Acid activation of clay minerals. *Dev. Clay Sci.* 2006, 1, 263–287. [https://doi.org/10.1016/S1572-4352\(05\)01008-1](https://doi.org/10.1016/S1572-4352(05)01008-1)
20. Rouquerol J., Llewellyn P., Sing K. Chapter 12. Adsorption by clays, pillared clays, zeolites and aluminophosphates. *Adsorption by powders and porous solids. Principles, methodology and applications.* 2nd ed. Amsterdam: Academic Press, 2014. P. 467–527. <https://doi.org/10.1016/B978-0-08-097035-6.00012-7>
21. Li T., Liu Y., Liu F.-S. Efficient preparation and application of palladium loaded montmorillonite as a reusable and effective heterogeneous catalyst for Suzuki cross-coupling reaction. *Appl. Clay Sci.* 2017, 136, 18–25. <https://doi.org/10.1016/j.clay.2016.11.004>
22. Guegan R., Gautier M., Beny J. M., Muller F. Adsorption of a C10E3 non-ionic surfactant on a Ca-smectite. *Clays Clay Miner.* 2009, 57(4), 502–509. <https://doi.org/10.1346/CCMN.2009.0570411>
23. Praus P., Turicova M. A. Physico-chemical study of the cationic surfactants adsorption on montmorillonite. *J. Braz. Chem. Soc.* 2007, 18(2), 378–383. <https://doi.org/10.1590/S0103-50532007000200020>
24. Krymova V. V., Filippovskiy S. S., Netreba E. E. Adsorbtsiya sulfonola na bentonitakh Krymskogo mestorozhdeniya [Adsorption of sulfonol on bentonites of the Crimean field]. *Uč. zap. Krym. fed. univ. imeni V. I. Vernadskogo. Biol. him.* [Scientific Notes of Crimean V. I. Vernadsky Federal University. Series Biology, Chemistry]. 2018, 4[70](4), 302–310. [in Russian].
25. Gammoudi S., Frini-Srasra N., Srasra E. Influence of exchangeable cation of smectite on HDTMA adsorption: equilibrium, kinetic and thermodynamic studies. *Appl. Clay Sci.* 2012, 69, 99–107. <https://doi.org/10.1016/j.clay.2011.11.011>
26. Shen T., Gao M. Gemini surfactant modified organo-clays for removal of organic pollutants from water: a review. *Chem. Eng. J.* 2019, 375, 121910. <https://doi.org/10.1016/j.cej.2019.121910>
27. Ni X., Li Z., Wang Y. Adsorption characteristics of anionic surfactant sodium dodecylbenzene sulfonate on the surface of montmorillonite minerals. *Front. Chem.* 2018, 6, 390–399. <https://doi.org/10.3389/fchem.2018.00390>
28. Wang Z. The adsorption of organic pollutants by Gemini surfactant-modified montmorillonite from water. *Mod. Approaches Oceanogr. Petrochem. Sci.* 2018, 1(2), 9–16. <https://doi.org/10.32474/MAOPS.2018.01.000106>
29. Korzh E. A., Klymenko N. A. Modelirovaniye kinetiki adsorbtsii farmatsevticheskikh veshchestv na aktivnykh uglyakh [Kinetic adsorption modeling of pharmaceuticals on activated carbons]. *Voda i vodoočisni tehnol.* [Water and Water Purification Technologies]. 2018, 22(1), 29–38. <https://doi.org/10.20535/2218-93002212018144240> [in Russian].
30. Abramzon A. A., Zaychenko L. P., Fayngol'ts S. I. Poverkhnostno-aktivnye veshchestva: sintez, analiz, svoystva, primeneniye: uchebnoe posobie dlya vuzov [Surfactants: synthesis, analysis, properties, application: study guide for higher education institutions]. Leningrad: Khimiya, 1988. 200 p. [in Russian].
31. Vafakhah S., Bahrololoom M. E., Saedikhani Mohsen S. K. Adsorption kinetics of cupric ions on mixture of modified corn stalk and modified tomato waste. *J. Water Resour. Prot.* 2016, 8(13), 1238–1250. <https://doi.org/10.4236/jwarp.2016.813095>

32. Ho Y. S., McKay G. Pseudo-second order model for sorption processes. *Process Biochem.* 1999, 34(5), 451–465. [https://doi.org/10.1016/S0032-9592\(98\)00112-5](https://doi.org/10.1016/S0032-9592(98)00112-5)
33. Weber W. J., Morris J. C. Kinetics of adsorption on carbon from solutions. *J. Sanit. Eng. Div. ASCE.* 1963, 89, 31–60.
34. Edwards P. M. Origin 7.0: scientific graphing and data analysis software. *J. Chem. Inf. Comput. Sci.* 2002, 42(5), 1270–1271. <https://doi.org/10.1021/ci0255432>
35. Wang J., Guo X. Adsorption isotherm models: classification, physical meaning, application and solving method. *Chemosphere.* 2020, 258, 127279. <https://doi.org/10.1016/j.chemosphere.2020.127279>
36. Hildebrand J. H., Scott R. L. The solubility of nonelectrolytes. New York: Reinhold Publishing Corporation, 1950. 488 p.

Стаття надійшла до редакції 03.11.2025

Стаття прийнята до друку після рецензування 13.11.2025

Стаття опублікована 29.12.2025

О. О. Стрельцова, Г. М. Джига, А. Ф. Тимчук

Одеський національний університет імені І. І. Мечникова,
кафедра фізичної та колоїдної хімії,
вул. Змієнка Всеволода, 2, м. Одеса, 65082, Україна;
e-mail: Tymchuk@onu.edu.ua

ДОСЛІДЖЕННЯ МЕХАНІЗМУ АДСОРБЦІЇ КАТІОННИХ ПОВЕРХНЕВО-АКТИВНИХ РЕЧОВИН БЕНТОНІТОМ АСКАНСЬКОГО РОДОВИЩА

Досліджено адсорбцію катіонних поверхнево-активних речовин — додециламонію хлориду та гексадецилпіридинію перхлорату з водних розчинів природним бентонітом Асканського родовища Грузії. Метою досліджень було з'ясування закономірностей та механізму процесу адсорбції досліджуваних катіонних поверхнево-активних речовин. Для порівняння адсорбційної здатності поверхнево-активних речовин бентонітом було використано константи адсорбції рівнянь Ленгмюра, Фрейндліха та Дубініна-Радушкевича. Результати показали, що після адсорбції катіонних поверхнево-активних речовин природним бентонітом не спостерігається особливих змін та утворення нових фаз за рахунок молекул поверхнево-активних речовин, що пов'язано з низьким вмістом цих речовин. Ступінь адсорбції залежить від концентрації поверхнево-активної речовини. Найвище значення (80%) було досягнуто для додециламонію хлориду з початковою концентрацією 50 мг/л. Отримані високі значення вільної енергії Гіббса адсорбції свідчать про високу спорідненість катіонних поверхнево-активних речовин до бентоніту. Кінетику процесу адсорбції було проаналізовано за допомогою кінетичних моделей псевдопершого та псевдодругого порядку, внутрішньоплівкової дифузії, внутрішньочастинкової дифузії Бойда та Вебера-Морріса.

Поглинання поверхнево-активних речовин глинами можна пояснити двома процесами: адсорбцією на поверхні глини та інтеркаляцією в шари глини. Це було підтверджено рентгеноструктурним аналізом та ІЧ-спектроскопією. На основі обробки експериментальних даних в рамках моделей хімічної кінетики та дифузії, а також рівнянь адсорбції Ленгмюра, Фрейндліха та Дубініна-Радушкевича було запропоновано механізм адсорбції досліджуваних поверхнево-активних речовин. Розрахунки показали, що процес адсорбції відповідає кінетичній моделі псевдодругого порядку. Процес відбувається в області змішаної дифузії, контрольованої як внутрішньою, так і зовнішньою дифузійною, що зумовлено шаруватою структурою адсорбенту. Аналіз даних за допомогою моделей адсорбції показав, що моделі Ленгмюра та Дубініна-Радушкевича краще інтерпретують експериментальні дані, ніж модель Фрейндліха. Процес адсорбції, проведений за оптимальних умов, забезпечує високий ступінь поглинання поверхнево-активних речовин. На основі отриманих даних можна зробити висновок, що природний бентоніт

Асканського родовища є високоефективним та придатним для спільного використання з катіонними поверхнево-активними речовинами у препаратах з антимікробними властивостями.

Ключові слова: катіонна поверхнево-активна речовина, бентоніт, адсорбція, кінетика.

СПИСОК ЛІТЕРАТУРИ

1. Parfitt G. D., Rochester C. H. Adsorption from solution at the solid/liquid interface. London: Academic Press, 1983. 416 p.
2. Sajid M., Nazal M., Baig N., Osman A. M. Removal of heavy metals and organic pollutants from water using dendritic polymers based adsorbents: a critical review. *Sep. Purif. Technol.* 2018, 191, 400–423. <https://doi.org/10.1016/j.seppur.2017.09.011>
3. Siyal A. A., Shamsuddin M. R., Low A., Rabat N. E. A review on recent developments in the adsorption of surfactants from wastewater. *J. Environ. Manage.* 2020, 254, 109797. <https://doi.org/10.1016/j.jenvman.2019.109797>
4. Awad A. M., Shaikh S. M., Jalab R., Gulied M. H., Nasser M. S., Benamor A., Adham S. Adsorption of organic pollutants by natural and modified clays: a comprehensive review. *Sep. Purif. Technol.* 2019, 228, 115719. <https://doi.org/10.1016/j.seppur.2019.115719>
5. Ying G. G., Guang-Guo Y. Fate, behaviour and effects of surfactants and their degradation products in the environment. *Environ. Int.* 2006, 32(3), 417–431. <https://doi.org/10.1016/j.envint.2005.07.004>
6. Seweryn A. Interactions between surfactants and the skin – Theory and practice. *Adv. Colloid Interface Sci.* 2018, 256, 242–245. <https://doi.org/10.1016/j.cis.2018.04.002>
7. Rosen M. J., Kunjappu J. M. Surfactants and interfacial phenomena. Hoboken, NJ: Jon Willey and Sons, Inc., 2012. 616 p.
8. Andrunik M., Bajda T. Modification of bentonite with cationic and nonionic surfactants: structural and textural features. *Materials.* 2019, 12(22), 3772. <https://doi.org/10.3390/ma12223772>
9. Shen T., Gao M. Gemini surfactant modified organo-clays for removal of organic pollutants from water. *Chem. Eng. J.* 2019, 375, 121910. <https://doi.org/10.1016/j.cej.2019.121910>
10. Khan M. N., Zareen U. Sand sorption process for the removal of sodium dodecyl sulfate (anionic surfactant) from water. *J. Hazard. Mater.* 2006, 133(1–3), 269–275. <https://doi.org/10.1016/j.jhazmat.2005.10.031>
11. Junin R., Amirian T., Idris A. K. Adsorption of nonionic surfactants on clay minerals. *J. Teknol.* 2011, 56(1), 113–122. <https://doi.org/10.11113/jt.v56.904>
12. Тарасевич Ю. Т., Овчаренко Ф. Д. Адсорбция на глинистых минералах. Киев: Наукова думка, 1975. 352 с.
13. Yang K., Zhu L., Xing B. Sorption of sodium dodecylbenzene sulfonate by montmorillonite. *Environ. Pollut.* 2007, 145(2), 571–576. <https://doi.org/10.1016/j.envpol.2006.04.024>
14. Li N., Xu L., Xu G., Sun W., Yu S. Simple synthesis of Cu₂O/Na-bentonite composites and their excellent photocatalytic properties in treating methyl orange solution. *Ceram. Int.* 2016, 42(5), 5979–5984. <https://doi.org/10.1016/j.ceramint.2015.12.145>
15. Vinuth M., Naik H. S. B., Vinoda B. M., Gururaj H., Thomas N., Arunkumar G. Enhanced removal of methylene blue dye in aqueous solution using eco-friendly Fe(III)–montmorillonite. *Mater. Today Proc.* 2017, 4(2A), 424–433. <https://doi.org/10.1016/j.matpr.2017.01.041>
16. Hong R., Guo Z., Gao J., Gu C. Rapid degradation of atrazine by hydroxyl radical induced from montmorillonite templated subnano-sized zero-valent copper. *Chemosphere.* 2017, 180, 335–342. <https://doi.org/10.1016/j.chemosphere.2017.04.025>
17. Khataee A., Kiransan M., Karaca S., Sheydaei M. Photocatalytic ozonation of metronidazole by synthesized zinc oxide nanoparticles immobilized on montmorillonite. *J. Taiwan Inst. Chem. Eng.* 2017, 74, 196–204. <https://doi.org/10.1016/j.jtice.2017.02.014>
18. Sánchez-Martín M. J., Dorado M. C., Del Hoyo C., Rodríguez-Cruz M. S. Influence of clay mineral structure and surfactant nature on the adsorption capacity of surfactants by clays. *J. Hazard. Mater.* 2008, 150(1), 115–123. <https://doi.org/10.1016/j.jhazmat.2007.04.093>
19. Komadel P., Madejová J. Chapter 7.1. Acid activation of clay minerals. *Dev. Clay Sci.* 2006, 1, 263–287. [https://doi.org/10.1016/S1572-4352\(05\)01008-1](https://doi.org/10.1016/S1572-4352(05)01008-1)

20. Rouquerol J., Llewellyn P., Sing K. Chapter 12. Adsorption by clays, pillared clays, zeolites and aluminophosphates. *Adsorption by powders and porous solids. Principles, methodology and applications*. 2nd ed. Amsterdam: Academic Press, 2014. P. 467–527. <https://doi.org/10.1016/B978-0-08-097035-6.00012-7>
21. Li T., Liu Y., Liu F.-S. Efficient preparation and application of palladium loaded montmorillonite as a reusable and effective heterogeneous catalyst for Suzuki cross-coupling reaction. *Appl. Clay Sci.* 2017, 136, 18–25. <https://doi.org/10.1016/j.clay.2016.11.004>
22. Guegan R., Gautier M., Beny J. M., Muller F. Adsorption of a C10E3 non-ionic surfactant on a Ca-smectite. *Clays Clay Miner.* 2009, 57(4), 502–509. <https://doi.org/10.1346/CCMN.2009.0570411>
23. Praus P., Turicova M. A. Physico-chemical study of the cationic surfactants adsorption on montmorillonite. *J. Braz. Chem. Soc.* 2007, 18(2), 378–383 <https://doi.org/10.1590/S0103-50532007000200020>
24. Крымова В. В., Филипповский С. С., Нетреба Е. Е. Адсорбция сульфанола на бентонитах Крымского месторождения. *Ученые записки Крымского федерального университета имени В. И. Вернадского. Биология, химия*. 2018, 4[70](4), 302–310.
25. Gammoudi S., Frini-Srasra N., Srasra E. Influence of exchangeable cation of smectite on HDTMA adsorption: equilibrium, kinetic and thermodynamic studies. *Appl. Clay Sci.* 2012, 69, 99–107. <https://doi.org/10.1016/j.clay.2011.11.011>
26. Shen T., Gao M. Gemini surfactant modified organo-clays for removal of organic pollutants from water: a review. *Chem. Eng. J.* 2019, 375, 121910. <https://doi.org/10.1016/j.cej.2019.121910>
27. Ni X., Li Z., Wang Y. Adsorption characteristics of anionic surfactant sodium dodecylbenzene sulfonate on the surface of montmorillonite minerals. *Front. Chem.* 2018, 6, 390–399. <https://doi.org/10.3389/fchem.2018.00390>
28. Wang Z. The adsorption of organic pollutants by Gemini surfactant-modified montmorillonite from water. *Mod. Approaches Oceanogr. Petrochem. Sci.* 2018, 1(2), 9–16. <https://doi.org/10.32474/MAOPS.2018.01.000106>
29. Корж Е. А., Клименко Н. А. Моделирование кинетики адсорбции фармацевтических веществ на активных углях. *Вода і водоочисні технології*. 2018, 22(1), 29–38. <https://doi.org/10.20535/2218-93002212018144240>
30. Абрамзон А. А., Зайченко Л. П., Файнгольд С. И. Поверхностно-активные вещества: синтез, анализ, свойства, применение: уч. пособ. для вузов. Ленинград: Химия, 1988. 200 с.
31. Yafakhah S., Bahrololoom M. E., Saedikhani Mohsen S. K. Adsorption kinetics of cupric ions on mixture of modified corn stalk and modified tomato waste. *J. Water Resour. Prot.* 2016, 8(13), 1238–1250. <https://doi.org/10.4236/jwarp.2016.813095>
32. Ho Y. S., McKay G. Pseudo-second order model for sorption processes. *Process Biochem.* 1999, 34(5), 451–465. [https://doi.org/10.1016/S0032-9592\(98\)00112-5](https://doi.org/10.1016/S0032-9592(98)00112-5)
33. Weber W. J., Morris J. C. Kinetics of adsorption on carbon from solutions. *J. Sanit. Eng. Div. ASCE.* 1963, 89, 31–60.
34. Edwards P. M. Origin 7.0: scientific graphing and data analysis software. *J. Chem. Inf. Comput. Sci.* 2002, 42(5), 1270–1271. <https://doi.org/10.1021/ci0255432>
35. Wang J., Guo X. Adsorption isotherm models: classification, physical meaning, application and solving method. *Chemosphere.* 2020, 258, 127279. <https://doi.org/10.1016/j.chemosphere.2020.127279>
36. Hildebrand J. H., Scott R. L. The solubility of nonelectrolytes. New York: Reinhold Publishing Corporation, 1950. 488 p.

ORCID iDs

- O. O. Streltsova: <https://orcid.org/0000-0002-2711-9314>
G. M. Dzhyga: <https://orcid.org/0000-0001-9971-7551>
A. F. Tymchuk: <https://orcid.org/0000-0001-6072-4869>